Polymer Chemistry

Self-assembly behavior of thermoresponsive difunctionalized γ-amide polycaprolactone amphiphilic diblock copolymers

Journal:	*Polymer Chemistry*
Manuscript ID	PY-ART-11-2022-001444.R1
Article Type:	Paper
Date Submitted by the Author:	17-Dec-2022
Complete List of Authors:	Stefan, Mihaela; The University of Texas at Dallas, Chemistry and Biochemistry Wang, Hanghang; University of Texas at Dallas, Chemistry Calubaquib, Erika; The University of Texas at Dallas, Chemistry and Biochemistry Bhadran, Abhi; The University of Texas at Dallas, Chemistry and Biochemistry Ma, Ziyuan; The University of Texas at Dallas, Chemistry and Biochemistry Miller, Justin; The University of Texas at Dallas, Chemistry and Biochemistry Zhang, Anyue ; The University of Texas at Dallas, Chemistry and Biochemistry Biewer, Michael; University of Texas at Dallas, Department of Chemistry

ARTICLE

Self-assembly behavior of thermoresponsive difunctionalized γ-amide polycaprolactone amphiphilic diblock copolymers

Received 00th January 20xx,
Accepted 00th January 20xx

DOI: 10.1039/x0xx00000x

Hanghang Wang[a], Erika L. Calubaquib[a], Abhi Bhadran[a], Ziyuan Ma[a], Justin T. Miller[a], Anyue Zhang[a], Michael C. Biewer[a], and Mihaela C. Stefan*[a]

Polycaprolactone (PCL)-based polymeric micelles are extensively used as drug delivery carriers to improve the bioavailability of poorly water soluble drugs due to their convenient tunability by varying functional groups on the polymers. An amide linkage enables the attachment of two different functional groups to the same position of PCLs, expanding the family of functional PCLs for drug delivery applications. In this work, a difunctionalized γ-amide ε-caprolactone (ε-CL) monomer (γ-ME_3PyCL) bearing a hydrophilic tri(ethylene glycol) (ME_3) group and a hydrophobic propyl group was synthesized. A homopolymer poly(*N*-propyl-*N*-(2-(2-(2-methoxyethoxy)ethoxy)ethyl)-7-oxoxepane-4-carboxamide) PME_3PyCL and three amphiphilic diblock copolymers poly(γ-benzyloxy-ε-caprolactone)-*b*-poly(*N*-propyl-*N*-(2-(2-(2-methoxyethoxy)ethoxy)ethyl)-7-oxoxepane-4-carboxamide) (PBnCL-*b*-PME_3PyCL), polycaprolactone-*b*-poly(*N*-propyl-*N*-(2-(2-(2-methoxyethoxy)ethoxy)ethyl)-7-oxoxepane-4-carboxamide) (PCL-*b*-PME_3PyCL), and polycaprolactone-*b*-poly(γ-2-(2-(2-methoxyethoxy)ethoxy)ethoxy-ε-caprolactone) (PCL-*b*-PME_3CL) were prepared by ring opening polymerization (ROP) using the organocatalyst triazabicylo[4.4.0]dec-5-ene (TBD) and benzyl alcohol (BnOH) initator. The ME_3 group contributes to the thermoresponsivity of the polymers. The diblock copolymer PBnCL-*b*-PME_3PyCL exhibited the most stable reversible phase transition due to enhanced π-π stacking interactions from the benzyl groups. All three diblock copolymers formed thermodynamically stable spherical micelles with low critical micelle concentration. A natural polyphenol, quercetin (Que) was used as hydrophobic cargo for loading. Among the three diblock polymers, PBnCL-*b*-PME_3PyCL exhibited the highest loading capacity due to enhanced π-π interactions between benzyl groups and Que.

Introduction

Polymeric micelles are excellent candidates for delivering poorly water-soluble drugs due to the convenient preparation of micelles and the versatile synthesis of amphiphilic polymers.[1-3] In aqueous media, amphiphilic polymers self-assemble to form core-shell structured micelles above the critical micelle concentration (CMC). The hydrophobic segments generate the hydrophobic micellar core, and the hydrophilic segments form the hydrophilic micellar shell. A desired CMC for drug delivery applications is close to 10^{-4}-10^{-3} g/L.[4] In this range, polymeric micelles are thermodynamically stable and can maintain their form in the bloodstream upon dilution without falling apart. Various amphiphilic polymers, such as homopolymers and block copolymers, have been used to prepare micelles for drug delivery applications.

Considering the clearance of the carrier materials from the body, extensive efforts have been made to develop biodegradable PCL-based amphiphilic diblock copolymers for micellar drug delivery.[4-7] The properties of PCL-based micelles can be tuned by varying the substituents on the diblock polymers. Yan et al.[8] synthesized amphiphilic diblock copolymer monomethoxy-poly(ethylene glycol)-*b*-poly[(ε-caprolactone-*co*-γ-(carbamic acid benzyl ester)-ε-caprolactone] (PEG-*b*-P(CL-*co*-CABCL)) bearing a hydrophobic carbamic acid benzyl ester (CAB) group and investigated the micellar delivery of poorly water-soluble anticancer drug doxorubicin (Dox). This diblock copolymer showed lower CMC in the range of 0.69-0.72 × 10^{-3} g/L and higher Dox loading capacity than the unfunctionalized diblock copolymer PEG-*b*-PCL. Soltantabar and Calubaquib et al.[9] reported the micellar delivery of Dox using fully biodegradable amphiphilic diblock copolymers PME_xCL-*b*-PBnCL (x = 2, 3, 4) bearing hydrophilic oligo(ethylene glycol) groups (ME_x) and hydrophobic benzyloxy group (Bn). The CMC of the diblock copolymers was in the range of 4.9-5.8 ×10^{-5} g/L.[9] The oligo(ethylene glycol) (OEG) groups also contribute to the thermoresponsivity of the polymers. Thermoresponsive polymers undergo coil-to-globule phase transition when the temperature is above their lower critical solution temperature (LCST) and become less souble in aqueous solutions. These OEG-fundiblock copolymers showed lower critical solution temperature (LCST) in the range of 15-59 °C. They facilitated the thermo-controlled release of micellar cargos when the external temperature was above their LCST. The desired LCST for drug delivery is a bit above body temperature. Hao et al.[10] reported a series of PME_3CL-based fully biodegradable amphiphilic

[a] Department of Chemistry and Biochemistry, University of Texas at Dallas, Richardson, TX, USA.
* Corresponding author; E-mail: mihaela@utdallas.edu
Electronic Supplementary Information (ESI) available: [details of any supplementary information available should be included here]. See DOI: 10.1039/x0xx00000x

diblock copolymers with proper CMC (1.92-8.95 × 10^{-3} g/L) and LCST (37-40 °C) for the delivery of Dox. Notably, amphiphilic diblock copolymers can form thermodynamic stable micelles. Thermoresponsive micelles for controlled drug release can also be obtained using OEG-functionalized polymers. However, it requires different types of monomers for sequential monomer addition to preparing the amphiphilic diblock copolymers.

In comparison, the synthesis of amphiphilic homopolymers is more straightforward by homopolymerizing one type of monomers. Basu[11] and Savariar[12] et al. synthesized amphiphilic alkene derivative monomers are incorporating a hydrophobic alkyl group and a hydrophilic carboxylic group through a rigid benzene linker or a flexible amide linker. Corresponding amphiphilic homopolymers self-assembled to form micelles with critical aggregation concentration values ranging from 6×10^{-4}-7×10^{-3} g/L. Liu et al.[13] synthesized amphiphilic homopolymers by alkene derivative monomers bearing a hydrophilic *N*-isopropylamine group or a hydrophilic OEG group. The self-assembly of those homopolymers generated micelles or vesicles with CMC ranging from 1×10^{-3}-9.8×10^{-2} g/L. In comparison, amphiphilic homopolymers bearing both hydrophobic and hydrophilic side chains can form more thermodynamically stable micelles than amphiphilic homopolymers bearing only a hydrophilic side chain. This is probably because of the enhanced hydrophobicity of amphiphilic homopolymers resulting from the additional hydrophobic pendant.

However, those vinyl-based homopolymers are nondegradable. Calubaquib et al.[14] reported the micellar self-assembly of biodegradable γ-functionalized PCL homopolymers bearing OEG groups. The monofunctionalized homopolymers bearing only hydrophilic OEG side chains showed high CMC of about 10^{-1} g/L and are thermoresponsive. In comparison, the more hydrophobic difunctionalized γ-amide homopolymer bearing a hydrophilic tri(ethylene glylcol) group and a hydrophobic dodecyl group showed lower CMC of about 10^{-2} g/L. However, it is not thermoresponsive. Additionally, this difunctionalized γ-amide homopolymer exhibited a 2.2-4.4 times higher drug loading capacity than the monofunctionalized homopolymers. Even though the biodegradable OEG-functionalized PCL homopolymers did not show desired thermodynamic stability for drug delivery, the properties of the difunctionalized γ-amide homopolymer were tuned by adding an additional hydrophobic functional group through an amide linkage. Enhanced hydrophobicity of the homopolymer resulted in an increase in thermodynamic stability and drug loading capacity but a decrease of thermoresponsivity.

To take advantage of the amide linkage to expand the family of fully biodegradable PCL-based polymers for micellar drug delivery, a new difunctionalized γ-amide ε-CL monomer bearing a hydrophilic ME_3 group and a less hydrophobic propyl group (γ-ME_3PyCL) was synthesized. By reducing the hydrophobicity, we expected that the new homopolymer poly(*N*-propyl-*N*-(2-(2-(2-methoxyethoxy)ethoxy)ethyl)-7-oxoxepane-4-carboxamide) PME_3PyCL would be thermoresponsive. To obtain improved thermodynamic stability, PME_3PyCL-based amphiphilic diblock copolymers consisting of a hydrophilic PCL or a γ-benzyloxy functionalized PCL block (PBnCL) were prepared and investigated. A natural polyphenol, quercetin, was used as a hydrophobic cargo for loading.

Results and Discussion

The new difunctionalized γ-amide ε-CL monomer bearing a hydrophilic ME_3 group and a hydrophobic propyl group (γ-ME_3PyCL) was prepared through a three-step synthesis (Scheme 1). The starting material propylamine reacted with methoxytriethylene glycol tosylate (ME_3OTs) to produce a secondary amine followed by amidation and Baeyer-Villiger oxidation to generate the target monomer. The monomer was characterized by ^{1}H NMR, ^{13}C NMR, and MALDI-ToF (Fig. S1–S7, Supporting Information).

The homopolymer PME_3PyCL was prepared through ROP using organocatalyst TBD and BnOH initiator at room temperature under a nitrogen atmosphere (Scheme 2a). TBD was reported as an efficient ROP catalyst for γ-amide functionalized ε-CL monomers.[14, 15] Fully biodegradable amphiphilic diblock copolymers PBnCL-*b*-PME_3PyCL, PCL-*b*-PME_3PyCL, and PCL-*b*-PME_3CL (control) were prepared by sequential monomer addition (Scheme 2b and 2c) with a exeriment ratio of 45 to 55 between hydrophobic and hydrophilic

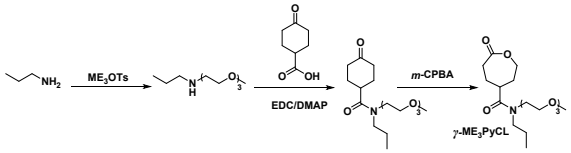

Scheme 1. Synthesis of difunctionalized γ-amide ε-CL monomer γ-ME_3PyCL.

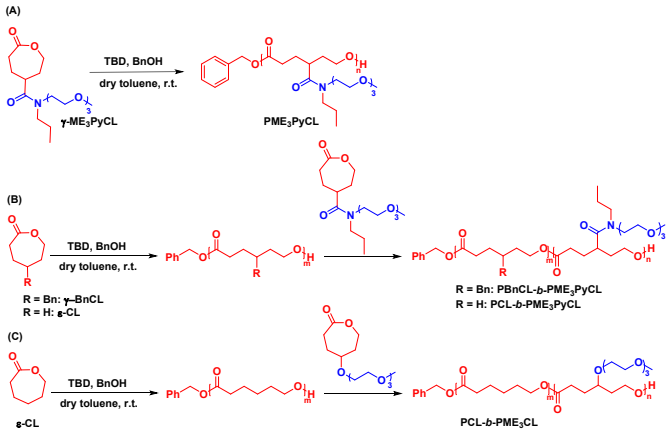

Scheme 2. Synthesis of (A) homopolymer poly(*N*-propyl-*N*-(2-(2-(2-methoxyethoxy)ethoxy)ethyl)-7-oxoxepane-4-carboxamide) (PME_3PyCL), and (B) amphiphilic diblock copolymers poly(γ-benzyloxy-ε-caprolactone)-*b*-poly(*N*-propyl-*N*-(2-(2-(2-methoxyethoxy)ethoxy)ethyl)-7-oxoxepane-4-carboxamide) (PBnCL-*b*-PME_3PyCL) and polycaprolactone-*b*-poly(*N*-propyl-*N*-(2-(2-(2-methoxyethoxy)ethoxy)ethyl)-7-oxoxepane-4-carboxamide) (PCL-*b*-PME_3PyCL), as well as (C) amphiphilic diblock copolymer polycaprolactone-*b*-poly(γ-2-(2-(2-methoxyethoxy)ethoxy)ethoxy-ε-caprolactone) (PCL-*b*-

PME_3CL). TBD: triazabicylo[4.4.0]dec-5-ene. BnOH: benzyl alcohol.

monomers. The γ-functionalized ε-CL monomers γ-ME_3CL and γ-BnCL were synthesized following the reported procedure in the literature.[9, 10] The synthesized polymers were characterized by ^1H NMR, ^{13}C NMR, and size exclusion chromatography (SEC) (Fig. S8-S16).

The molecular weights and compositions of the synthesized polymers are summarized in Table 1. The molecular weights estimated from ^1H NMR were calculated by multiplying the molecular weights of monomers with the degree of polymerization (DPn) of polymers and adding the molecular weight of the initiator. The DPn of homopolymer PME_3PyCL was estimated by the integration of methylene protons of the end group (at ~5.1 ppm) to the integration of methoxy protons of ME_3 substituent (at ~3.4 ppm). The DPn of amphiphilic diblock copolymer PBnCL-*b*-PME_3PyCL was estimated by the ratio of the integration of methylene protons of the end group (at ~5.1 ppm) to the integration of methoxy protons of ME_3 group on the hydrophilic block (at ~3.4 ppm) and the integration of methylene protons of benzyloxy substituent on the hydrophobic block (at ~4.5 ppm). The DPn of amphiphilic diblock copolymers PCL-*b*-PME_3PyCL and PCL-*b*-PME_3CL were estimated by the ratio of the integration of methylene protons of the end group (at ~5.1 ppm) to the integration of methoxy protons of ME_3 substituent on the hydrophilic block (at ~3.4 ppm) and the methylene protons adjacent to the oxygen on the hydrophobic block (at ~4.1 ppm). The molecular weights obtained from SEC are lower than those determined by ^1H NMR. This might be due to the difference in the hydrodynamic volume of the polymers and the poly (methyl methacrylate) (PMMA) standard used for calibration. The polydispersity (PDI) of polymers ranged from 1.38-1.87. Differential scanning calorimetry (DSC) (Fig. S17 and Table 1) demonstrated that the homopolymer PME_3PyCL and diblock copolymer PBnCL-*b*-PME_3PyCL are amorphous, while the diblock copolymers PCL-*b*-PME_3PyCL and PCL-*b*-PME_3CL are semicrystalline due to the semicrystalline PCL block.

The ME_3 functional group contributes to the thermoresponsivity of the monofunctionalized PME_3CL homopolymer, of which the LCST is 65.5 °C in water.[14] We hypothesized that the new difunctionalized γ-amide homopolymer PME_3PyCL would have a lower LCST due to the increased hydrophobicity from the additional hydrophobic propyl group. The LCST of the homopolymer PME_3PyCL was determined by thermo UV-Vis spectroscopy. Thermoresponsive polymers having an LCST can undergo phase transition when the external temperature is above their LCST, and the polymers become immiscible with the aqueous solutions due to dehydration. This leads to a decrease in UV-vis transmittance of the aqueous polymer solutions. In this work, a series of PME_3PyCL aqueous solutions with different polymer concentrations (1, 2.5, 5, and 10 mg/mL) were prepared by direct dissolution and equilibration for 24 hrs. The LCST was determined by the external temperature at which 50% drop in transmittance was observed (Fig. 1).

The thermoresponsivity of homopolymer PME_3PyCL was first investigated in water. The plots of transmittance *vs.* temperature (Fig. 1A) and the turbidity curves (Fig. S18) demonstrated that the phase transition in heating and cooling cycles was reversible. The LCST obtained from the cooling cycle is slightly lower (1.4-1.7 °C) than that from the heating cycle (Table. S1). This is probably because the dehydrated ME_3 units have to overcome the energy barrier (such as weak intramolecular and intermolecular *van der Waals* interactions) to become rehydrated; therefore, it results in hysteresis.[14, 16-19] Notably, the LCST of homopolymer PME_3PyCL in water increases with the decrease of polymer concentration (Fig. 1C). The LCST values are 35.3 °C, 36.9 °C, 39.0 °C, 41.5 °C at polymer concentrations of 10 mg/mL, 5 mg/mL, 2.5 mg/mL, and 1 mg/mL, respectively (Table S1). Similar observations were reported for thermoresponsive polymers such as OEG-substituted polysulfides,[16] OEG-substituted polyacrylates,[20] OEG-substituted polystyrenics,[20] PEG-DTPA,[21] Pluronic L62,[22] PDMDOMA,[23] PNASME,[24] and PNiPAm-*b*-PEtOx-*b*-PNiPAm.[25] At a lower polymer concentration, the homopolymer PME_3PyCL is more dispersed in water. The limited intermolecular interactions may contribute to a delayed phase transition; therefore, a higher LCST was obtained at a lower polymer concentration.[14, 16, 21] Additionally, the characterization technique may be limited at low polymer concentrations, leading to delayed detection of phase transition.[14, 26] Compared to the reported LCST of PME_3CL homopolymer,[14] the LCST of PME_3PyCL is substantially decreased due to its increased hydrophobicity from the additional hydrophobic propyl group. Meanwhile, the thermoresponsivity of PME_3PyCL was improved in comparison with that of the difunctionalized γ-amide PCL homopolymer bearing a more hydrophobic dodecyl group.[14] The hydrophobicity of the homopolymers affects their thermoresponsivity, and the LCST of the homopolymers increases with a decrease of their hydrophobicity.

Table 1. Molecular weights and composition of diblock copolymers

Polymers	Experiment ratio[a]	mol% Hydrophobic : Hydrophilic [b]	M_n (kg/mol)$^{NMR, c}$	M_n (kg/mol)$^{SEC, d}$	$PDI^{SEC, d}$	T_g (^oC)[e]	T_m (^oC)[e]
PME_3PyCL	0 : 55 : 1 : 1	--	23.3	5.6	1.87	-44.4	--
PBnCL-*b*-PME_3PyCL	45 : 55 : 1 : 1	47 : 53	27.6	8.7	1.49	-35.6	--
PCL-*b*-PME_3PyCL	45 : 55 : 1 : 1	47 : 53	19.8	5.3	1.69	-48.4	49.5
PCL-b-PME_3CL	45 : 55 : 1 : 1	44 : 56	24.6	6.0	1.38	-67.5	36.7

[a] Exeriment ratio of hydrophobic monomer : hydrophilic monomer : TBD catalyst : BnOH initiator; [b] Determined by ^1H NMR; [c] Determined by ^1H NMR by multiplying the degree of polymerization of the polymer with the molecular weight of the monomer repeating unit then adding the molecular weight of the end group. The degree of polymerization was estimated from the ratio of the integrations of the methylene benzyl protons of the initiator, the methoxy group of ME_3 substituent on the hydrophilic block, and the methylene protons adjacent to the oxygen on the hydrophobic block backbone/ the methylene protons of benzyloxy substituent on the hydrophobic block. [d] Determined by size exclusion chromatography using PMMA standard. [e] Determined by differential scanning calorimetry.

ARTICLE

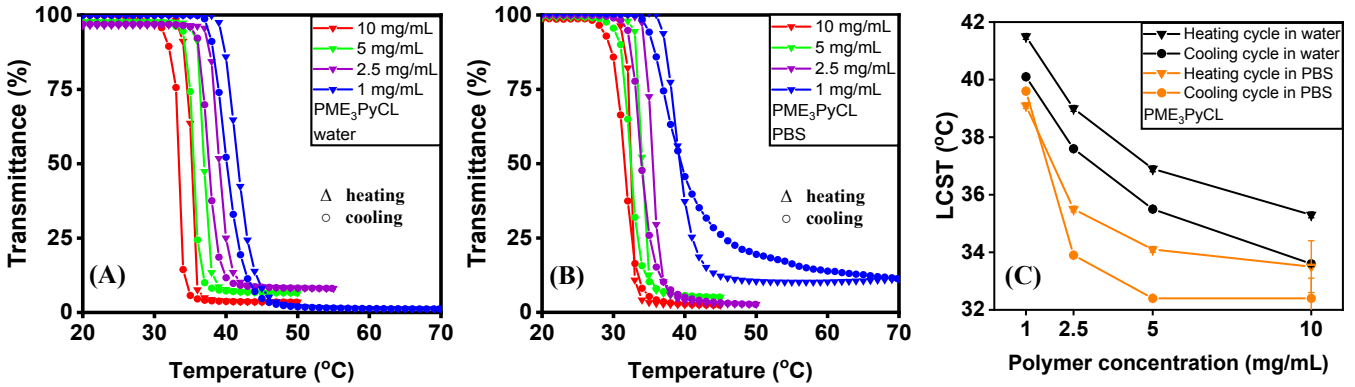

Fig. 1 (A, B, and C). UV-Vis transmittance *vs.* temperature spectra obtained from aqueous solutions of the homopolymer PME_3PyCL (Δ is heating and ○ is cooling): (A) in DI water, and (B) in PBS (1×, pH = 7.4). (C) Polymer concentration *vs.* LCST curves (n = 3).

Salt additives affect the thermal behaviors of thermoresponsive polymers.[19, 23, 27-34] The salts in buffer solutions might have a significant impact on the behavior of thermoresponsive polymers used in drug delivery applications. Therefore, the LCST of homopolymer PME_3PyCL in phosphate-buffered saline (PBS, 1×, pH = 7.4), a commonly used buffer solution for biological research, was investigated. The PBS (1×, pH = 7.4) was prepared by diluting commercially available PBS (10×) solution with Milli-Q water, and its composition is NaCl 137 mM, KCl 2.7 mM, and 11.9 mM phosphates. We hypothesized that the salt additives would decrease the LCST of homopolymer PME_3PyCL, because chloride and phosphate slats were reported to decrease the phase transition temperatures of PEG,[31] poly(2-(2-methoxyethoxy)ethyl methacrylate-*co*-oligo(ethylene glycol) methacrylate) (P(MEO_2MA-*co*-OEGMA)),[19] poly(propylene oxide) (PPO),[28] and poly(oligo(ethylene glycol) methyl ether methacrylate-*co*-2,2,2,-trifluoroethyl acrylate) (poly(OEGMA-*co*-TFEA)).[33] Additionally, Chen et al. [16] reported that the LCST of OEG-substituted polysulfides in PBS were lower than those in DI water.

Figure 1C demonstrates that the LCST of homopolymer PME_3PyCL in PBS is lower than in DI water. This can be attributed to the partial dehydration of PME_3PyCL caused by salt additives, and it results in a salting-out effect and the decrease of LCST.[19] The phase transition of PME_3PyCL in PBS (1×, pH = 7.4) is reversible (Fig. 1B and Fig. S19), and the LCST of PME_3PyCL in PBS are 33.5 °C, 34.1 °C, 35.5 °C, and 39.6 °C at polymer concentrations of 10 mg/mL, 5 mg/mL, 2.5 mg/mL, and 1 mg/mL, respectively (Table S2). The LCST of PME_3PyCL in PBS also increases as polymer concentration decreases. Hysteresis was also observed in PBS. A slightly lower (1.1-1.7 °C) LCST was obtained in the cooling cycle than in heating cycle in PBS at polymer concentrations of 10 mg/mL, 5 mg/mL, and 2.5 mg/mL, while the LCST of the cooling cycle and heating cycle at a polymer concentration of 1 mg/mL are almost the same (Fig. 1C and Table S2).

The new homopolymer PME_3PyCL is thermoresponsive, and its LCST is close to the physiological temperature. However, it is unlikely to self-assemble to form stable thermodynamic micelles with the desired CMC (10^{-4}-10^{-3} g/L) for drug delivery applications.[4] Compared to the reported difunctionalized γ-amide PCL homopolymer bearing a dodecyl hydrophobic group,[14] the PME_3PyCL homopolymer is less hydrophobic and may lead to a higher CMC. To understand the thermodynamic stability of polymeric micelles in physiological conditions, the CMC of PME_3PyCL was determined using pyrene as a fluorescence probe in PBS (1×, pH = 7.4).[35] A series of aqueous polymer solutions in PBS with various polymer concentrations and a constant concentration of pyrene were prepared. Pyrene exhibits different excitation wavelengths in a hydrophobic environment and a hydrophilic environment. When polymeric micelles are formed above their CMC, the dispersed pyrene in an aqueous solution can be encapsulated in the hydrophobic micellar core resulting in a shift in the excitation spectrum. The CMC was determined by the polymer concentration at which an abrupt change in the ratio of excitation peak intensities at 338 nm and 334 nm (i.e., I_{338}/I_{334}) was observed. The CMC of PME_3PyCL is 6.39×10^{-2} g/L (Fig. S20).

To obtain thermodynamically stable micelles, amphiphilic diblock copolymers PBnCL-*b*-PME_3PyCL and PCL-*b*-PME_3PyCl as well as a control sample of PCL-*b*-PME_3CL were prepared. The PBnCL was chosen as a hydrophobic block considering enhanced drug loading capacity due to π-π stacking interactions between the benzyl group with hydrophobic cargos.[8, 9, 36-38] The CMC of the synthesized amphiphilic diblock copolymers was

also determined in PBS (1×, pH = 7.4) using pyrene as a fluorescence probe (Fig. 2A-C). The CMC values of PBnCL-*b*-PME_3PyCL, PCL-*b*-PME_3PyCL, and PCL-*b*-PME_3CL are 1.07×10^{-3} g/L, 8.37×10^{-3} g/L, and 6.97×10^{-3} g/L. All three amphiphilic diblock copolymers have desired CMC, and the CMC of PCL-*b*-PME_3CL in PBS is comparable to the reported CMC in water (1.20×10^{-3} g/L).[39]

The thermoresponsivity of amphiphilic diblock copolymers PBnCL-*b*-PME_3PyCL, PCL-*b*-PME_3PyCL, and PCL-*b*-PME_3CL was investigated in PBS (1×, pH = 7.4), considering the influence of salts on the thermal behavior of polymers. PBnCL-*b*-PME_3PyCL diblock copolymer can completely dissolve in PBS (1×, pH = 7.4) at low polymer concentration (1 mg/mL) while PCL-*b*-PME_3PyCL and PCL-*b*-PME_3CL diblock copolymers could not. This might be attributed to the enhanced intermolecular/intramolecular π-π interactions from benzyl substituents of PBnCL-*b*-PME_3PyCL diblock copolymer, facilitating less exposure of hydrophobic components but more exposure of hydrophilic ME_3 units towards the water. However, PBnCL-*b*-PME_3PyCL is the most hydrophobic copolymer. When increasing the polymer concentration to 2.5 mg/mL, PBnCL-*b*-PME_3PyCL could not completely dissolve in PBS, and the solution became turbid. The LCST of amphiphilic diblock copolymers was characterized at a polymer concentration of 1 mg/mL. Considering the dissolution ability of polymers, transparent aqueous solutions of PCL-*b*-PME_3PyCL and PCL-*b*-PME_3CL were prepared by dialysis method, and PBnCL-*b*-PME_3PyCL aqueous solution was prepared by direct dissolution. The UV-Vis transmittance vs temperature plots (Fig. 2D-F) and turbidity curves (Fig. S21) demonstrated that PBnCL-*b*-PME_3PyCL has a sharper reversible phase transition than that of PCL-*b*-PME_3CL and the phase transition of PCL-*b*-PME_3PyCL is not reversible. Precipitation was observed from the PCL-*b*-PME_3PyCL aqueous solution after the thermoresponsivity test. The irreversible phase transition of PCL-*b*-PME_3PyCL diblock copolymer may be caused by the increased hydrophobicity due to the additional propyl substituent, compared to the PCL-*b*-PME_3CL diblock copolymer. However, the most hydrophobic PBnCL-*b*-PME_3PyCL diblock copolymer exhibited the best reversibility and stability during thermoresponsivity test. This is probably due to the amorphous nature of PBnCL block. Moreover, the intermolecular/intramolecular interactions between benzyl substituents provide more flexibility and stability to the PBnCL-*b*-PME_3PyCL diblock copolymer when undergoing a phase transition. While the semicrystalline PCL block makes the PCL-*b*-PME_3PyCL and PCL-*b*-PME_3CL diblock copolymers more rigid, and there are less intramolecular/intermolecular interactions. The LCST values of PBnCL-*b*-PME_3PyCL, PCL-*b*-PME_3PyCL, and PCL-*b*-PME_3CL are 28.6 °C, 30.9 °C, and 39.4 °C, respectively (Table S3). As the hydrophobicity of copolymers increases, the LCST values decrease.[40]

Empty micelles were prepared by dialysis method in PBS (1×, pH = 7.4). Briefly, a 0.6 mL THF solution of 2 mg amphiphilic diblock copolymer was added dropwise to 2 mL PBS (1×, pH = 7.4) while homogenizing. The mixture was transferred to a

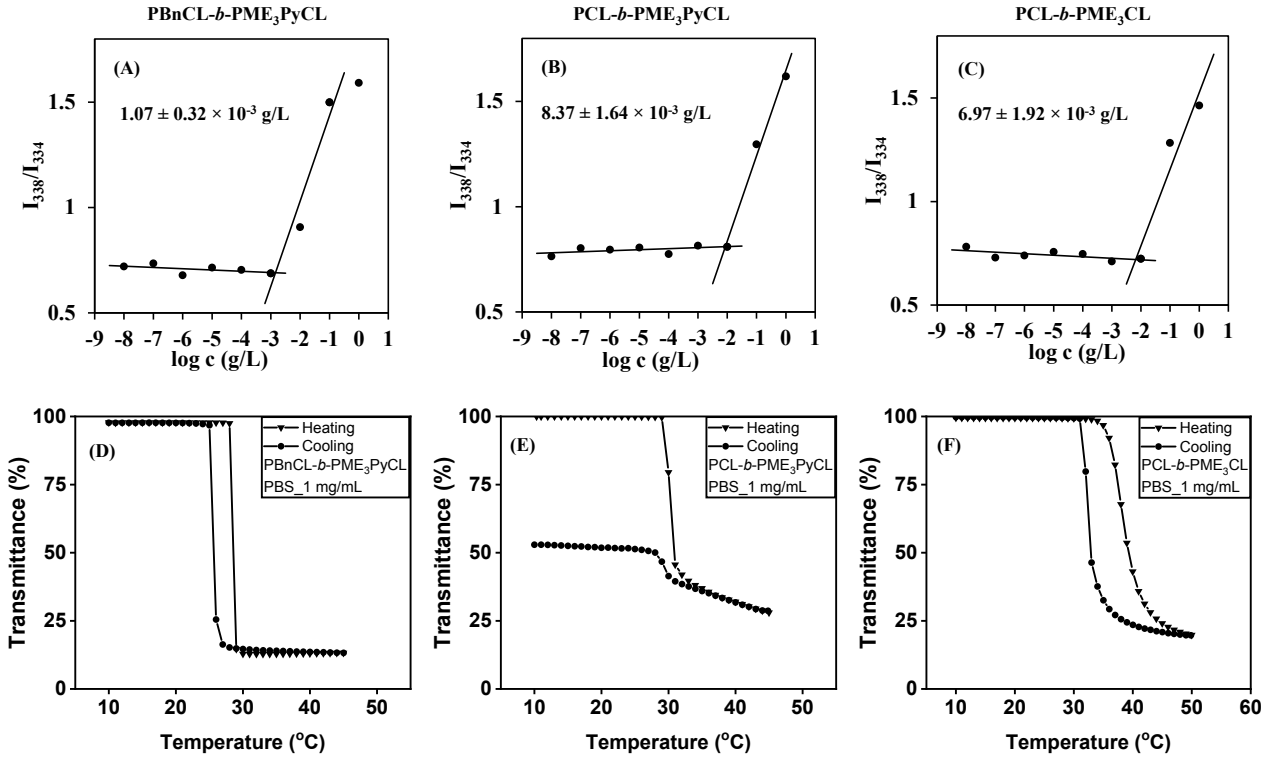

Fig. 2 (A-F). (A-C) CMC plots of amphiphilic diblock copolymers in PBS (1×, pH = 7.4) were determined using pyrene as a fluorescence probe. (D-F) UV-Vis transmittance *vs.* temperature plots obtained from aqueous solutions of the amphiphilic diblock copolymer in PBS (polymer concentration = 1 mg/mL) (▼ is heating and ● is cooling) (n =3).

ARTICLE

dialysis bag (MW cutoff: 3500 Da) for dialysis against 500 mL PBS (1×, pH = 7.4) for 24 hrs. Micelle solutions were obtained after filtration with a 0.45 μm nylon syringe filter. Empty micelle sizes were determined by DLS, and the morphology was characterized by TEM (Fig. 3). The micelles sizes of PBnCL-*b*-PME_3PyCL, PCL-*b*-PME_3PyCL, and PCL-*b*-PME_3CL are 32.71 nm, 30.43 nm, 86.82 nm, respectively. The smaller micelle sizes for PBnCL-*b*-PME_3PyCL and PCL-*b*-PME_3PyCL might be due to the enhanced interactions in the hydrophobic core from benzyl substituent and propyl substituent. The micelle size of PCL-*b*-PME_3CL in PBS is comparable to the reported micelle size in water (96.4 nm).[39] TEM images demonstrated that spherical micelles were formed. The micelle sizes determined from TEM for PBnCL-*b*-PME_3PyCL, PCL-*b*-PME_3PyCL, and PCL-*b*-PME_3CL are in ranges of 25-27 nm, 23-30 nm, and 60-82 nm, respectively. Smaller micelle sizes were obtained by TEM because the micelles were dehydrated during the TEM test. At the same time, they are hydrated in solutions for the DLS test.[9, 14, 41-43] Negative zeta potentials were obtained for all micelles. The values are comparable to the reported zeta potential of PCL-based block copolymer methoxy-poly(ethylene glycol) $_{2000}$-poly(2-(*N*,*N*-diethylamino)ethyl methacrylate)-polycaprolactone (mPEG-PDEA-PCL) in PBS.[44]

The possible use of PBnCL-*b*-PME_3PyCL, PCL-*b*-PME_3PyCL, and PCL-*b*-PME_3CL for drug delivery applications was investigated by loading hydrophobic quercetin (Que), a natural oxidant. Que has been proven to have anticancer properties, and its bioavailability is limited by poor water solubility.[9, 45-54] It is significant to develop drug carriers to improve the bioavailability of Que. The Que-loaded micelles were prepared by dialysis method in PBS (1×, pH = 7.4) first. Briefly, a 0.6 mL THF solution of 2 mg polymer and 0.2 mg Que was added to 2 mL PBS with homogenization. Then the mixture was dialyzed against 500 mL PBS for 24 hrs. Que-loaded micelle solutions were obtained after filtration with a 0.45 μm nylon syringe filter. Multimodal distributions were observed from DLS (Fig. S22). This might be due to a more severe salt-out

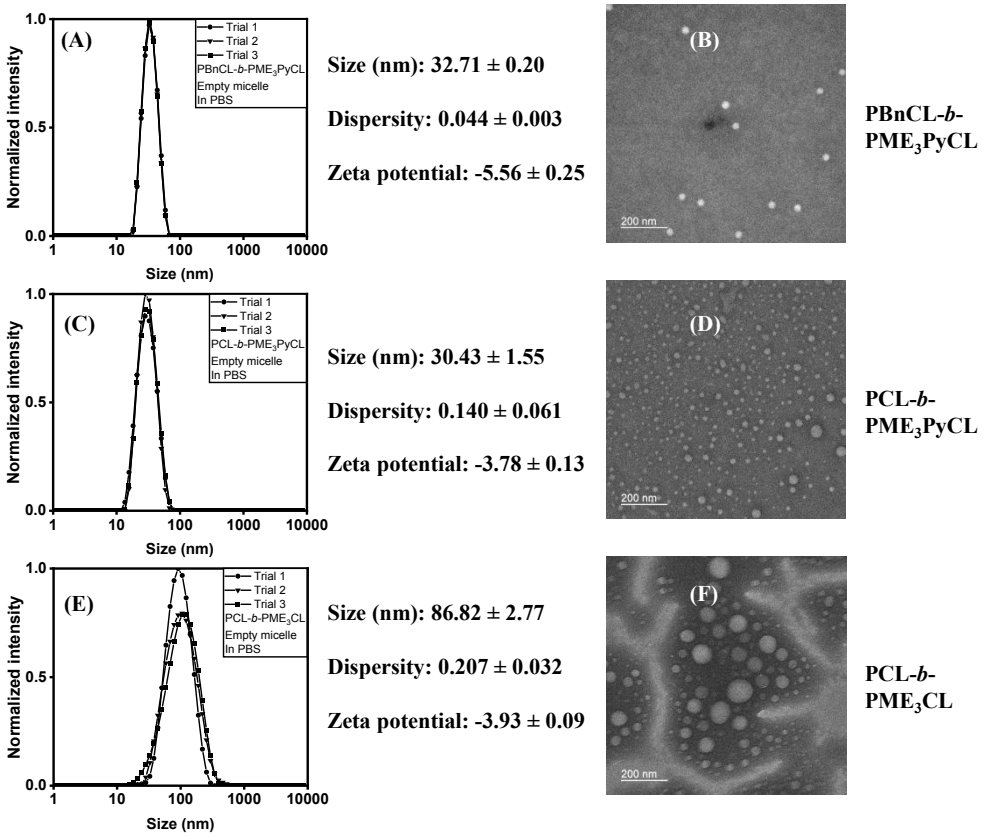

Fig. 3 (A-F). DLS (A, C, E) and TEM (B, D, F) of empty micelles prepared by self-assembly of amphiphilic diblock copolymers PBnCL-*b*-PME_3PyCL, PCL-*b*-PME_3PyCL, and PCL-*b*-PME_3CL in PBS (×1, pH = 7.4).

ARTICLE

effect due to additional hydrophobic Que influences polymer/drug precipitation and micelle formation. Que-loading was performed in water using the same dialysis method to confirm this. Monomodal distribution in DLS was observed for all three Que-loaded micelle solutions (Fig. 4A, 4C, 4E). The Que-loaded micelle sizes are 75.42nm, 86.77nm, and 76.64 nm for PBnCL-*b*-PME$_3$PyCL, PCL-*b*-PME$_3$PyCL, and PCL-*b*-PME$_3$CL, respectively (Table 2). TEM images showed spherical micelles were formed (Fig. 4B, 4D, 4F), with smaller sizes, as previously noted. All three Que-loaded micelles were tested to have negative zeta potential (Table 2). The values are comparable with those of PME$_3$CL-based eugenol-loaded micelles[14] and Dox-loaded micelles.[10] Que-loaded micelles were collapsed by DMSO, and the solutions were subjected to a UV-Vis spectrometer for an absorbance test. The Que concentration in solutions was determined by using a pre-plotted Que calibration curve (Fig. S23). Drug loading capacity (DLC) and drug loading efficiency (EE) were calculated. The DLC of PBnCL-*b*-PME$_3$PyCL, PCL-*b*-PME$_3$PyCL, and PCL-*b*-PME$_3$CL are 0.77%, 0.31%, and 0.40% (Table 2). As hypothesized, the PBnCL-*b*-PME$_3$PyCL had the highest loading capacity, which is 1.9-2.5 times higher than those of PCL-*b*-PME$_3$PyCL, and PCL-*b*-PME$_3$CL. The enhanced DLC of PBnCL-*b*-PME$_3$PyCL is attributed to π-π stacking between benzyl substituents and hydrophobic Que. The DLC of PCL-*b*-PME$_3$CL is comparable to the reported DLC of Dox.[39] The aqueous media can affect drug-loaded micelles preparation. To improve the self-assembly behaviors of difunctionalized γ-amide PCLs in PBS (1×, pH = 7.4), more hydrophilic OEG functional groups such as tetra oligo (ethylene glycol) can be used to replace the ME$_3$ group to enhance the solubility of polymers.

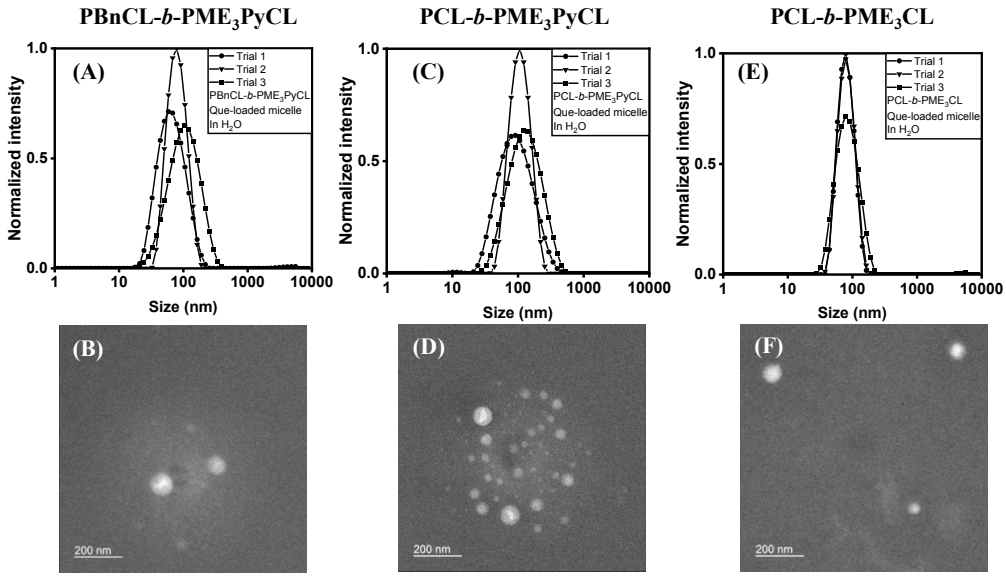

Fig. 4 (A-F). DLS (A, C, E) and TEM (B, D, F) of Que-loaded micelles of amphiphilic diblock copolymers PBnCL-*b*-PME$_3$PyCL, PCL-*b*-PME$_3$PyCL, and PCL-*b*-PME$_3$CL in water.

Table 2. Characteristics of Que-loaded micelles prepared in water.

Polymer	Size (nm) [a]	Dispersity [a]	Zeta potential [a]	DLC (wt %)	EE (wt%)
PBnCL-*b*-PME$_3$PyCL	75.42 ± 12.51	0.156 ± 0.055	- 18.0 ± 4.8	0.77 ± 0.13	7.73 ± 1.27
PCL-*b*-PME$_3$PyCL	86.77 ± 10.79	0.204 ± 0.078	- 16.7 ± 1.8	0.31 ± 0.10	5.01 ± 1.59
PCL-*b*-PME$_3$CL	76.64 ± 0.48	0.093 ± 0.043	- 16.6 ± 1.1	0.40 ± 0.06	3.98 ± 0.65

a Determined by DLS (n = 3).

ARTICLE

Conclusions

To conclude, a new difunctionalized γ-amide ε-CL monomer (γ-ME_3PyCL) bearing a hydrophilic ME_3 group and a hydrophobic propyl group was synthesized. The polymerization of γ-ME_3PyCL was achieved by ROP using organocatalyst TBD and BnOH initiator to generate thermoresponsive homopolymer PME_3PyCL. The LCST of the homopolymer is close to physiological temperature. Fully biodegradable amphiphilic diblock copolymers PBnCL-*b*-PME_3PyCL and PCL-*b*-PME_3PyCL, as well as a control PCL-*b*-PME_3CL are also thermoresponsive. Among the copolymers, PBnCL-*b*-PME_3PyCL exhibited the best reversibility due to enhanced π-π interactions from the benzyl substituents. All three diblock copolymer self-assembled to form thermodynamically stable micelles with low CMC. Among them, PBnCL-*b*-PME_3PyCL micelles showed the highest drug loading capacity due to enhanced π-π stacking interactions between the benzyl substituent and the hydrophobic cargo, quercetin. Fully biodegradable difunctionalized γ-amide amphiphilic diblock copolymers are excellent for preparing thermodynamically stable polymeric micelles for drug delivery applications. The amide linkage provides an excellent opportunity to tune the properties of the polymers by adding two functional groups.

Experimental Section

Synthesis

Monomer synthesis and characterization are shown in Supporting Information.

Synthesis of poly(N-propyl-N-(2-(2-(2-methoxyethoxy)ethoxy)ethyl)-7-oxoxepane-4-carboxamide) homopolymer, PME_3PyCL. To a Schlenk flask, organocatalyst triazabicylo[4.4.0]dec-5-ene (TBD) (9.4 mg, 0.06 mmol) and BnOH initiator (7.4 mg, 0.06 mmol) stock solution in dry toluene were added. After stirring for 0.5 hours in the glove box, the γ-ME_3PyCL monomer (1.14 g, 3.30 mmol) was added. The mixture was stirred in the glovebox at room temperature until the monomer was completely consumed. Then the polymerization was quenched by exposing it to air and acetic acid. The homopolymer PME_3PyCL was obtained by precipitation from THF/hexane. The monomer γ-ME_3PyCL was dried with calcium hydride before polymerization. PME_3PyCL: ^{1}H NMR (500 MHz, $CDCl_3$) δ: 0.85-0.90 (m, 3 H), 1.51-1.59 (m, 2H), 1.70-1.78 (m, 2H), 1.91-1.99 (m, 2H), 2.20-2.29 (m, 2H), 2.80-2.86 (d, 1H), 3.27-3.31 (m, 2H), 3.37 (s, 3H), 3.49-3.63 (m, 12H), 3.93-4.10 (m, 2H). ^{13}C NMR (500 MHz, $CDCl_3$) δ: 11.22, 11.38, 20.86, 20.97, 22.72, 31.22, 31.38, 31.55, 36.76, 37.69, 46.32, 46.90, 47.34, 48.30, 50.63, 59.01, 62.39, 62.59, 69.21, 69.50, 70.40, 70.51, 70.57, 70.63, 70.68, 71.90, 172.78, 172.80, 172.83, 172.85, 172.94, 173.95. SEC: Mn = 5600 gmol^{-1}, PDI = 1.87.

Synthesis of polycaprolactone-b-poly(N-propyl-N-(2-(2-(2-methoxyethoxy)ethoxy)ethyl)-7-oxoxepane-4-carboxamide) diblock copolymer, PCL-*b*-PME_3PyCL. To a Schlenk flask, organocatalyst TBD (9.4 mg, 0.06 mmol) and BnOH initiator (7.4 mg, 0.06 mmol) stock solution in dry toluene were added. After stirring for 0.5 hour in the glove box, the hydrophobic monomer ε-CL (308.2 mg, 2.7 mmol) was added. The mixture was stirred in the glovebox at room temperature until the monomer was completely consumed. Then the hydrophilic monomer γ-ME_3PyCL monomer (1.14 g, 3.30 mmol) was added. After the second monomer was fully converted, the polymerization was quenched by exposing it to air and acetic acid. The amphiphilic diblock copolymer was obtained by precipitating from THF/hexane. The monomers were dried with calcium hydride before polymerization. PCL-*b*-PME_3PyCL: ^{1}H NMR (500 MHz, $CDCl_3$) δ: 0.86-0.90 (m, 3H), 1.35-1.41 (m, 2H), 1.55-1.68 (m, 6H), 1.71-1.78 (m, 2H), 1.92-2.01 (m, 2H), 2.24-2.32 (m, 4H), 2.80-2.87 (d, 1H), 3.29-3.30 (d, 2H), 3.37 (s, 3H), 3.49-3.66 (m, 12H), 3.97-4.07 (m, 4H). ^{13}C NMR δ: 11.37, 11.53, 20.87, 21.01, 22.88, 24.73, 25.69, 27.76, 28.51, 31.37, 34.28, 36.92, 38.04, 46.48, 47.50, 50.79, 51.03, 59.17, 62.56, 64.30, 69.37, 69.65, 70.55, 70.66, 70.72, 70.78, 70.83, 72.06, 72.09, 173.68. SEC: Mn = 8700 gmol^{-1}, PDI = 1.49.

Synthesis of poly(γ-benzyloxy-ε-caprolactone)-b-poly(N-propyl-N-(2-(2-(2-methoxyethoxy)ethoxy)ethyl)-7-oxoxepane-4-carboxamide) diblock copolymer, PBnCL-b-PME_3PyCL. The same procedure was followed for the synthesis of PBnCL-*b*-PME_3PyCL with exeriment ratio [γ-BnCL]:[γ-ME_3PyCL]:[TBD]:[BnOH] = 45:55:1:1. ^{1}H NMR (500 MHz, $CDCl_3$) δ: 0.89-0.93 (m, 3H), 1.54-1.61 (m, 2H), 1.73-1.89 (m, 4H), 1.91-2.02 (m, 2H), 2.23-2.30 (m, 2H), 2.36-2.39 (t, 2H), 2.83-2.89 (d, 1H), 3.33-3.34 (m, 2H), 3.40 (s, 3H), 3.55-3.67 (m, 13H), 3.98-4.09 (m, 2H), 4.16-4.18 (t, 2H), 4.46-4.52 (m, 2H), 7.33-7.35 (m, 4H). ^{13}C NMR δ: 11.23, 11.38, 20.87, 22.72, 27.55, 28.77, 29.67, 31.23, 31.53, 32.85, 36.76, 46.33, 46.90, 47.34, 48.31, 50.64, 59.02, 61.25, 62.39, 69.22, 69.49, 70.40, 70.52, 70.57, 70.63, 70.68, 71.08, 71.91, 71.94, 74.60, 74.65, 127.67, 127.77, 128.39, 138.29, 173.39. SEC: Mn = 5300 gmol^{-1}, PDI = 1.69.

Synthesis of polycaprolactone-b- poly(γ-2-(2-(2-methoxyethoxy)ethoxy)ethoxy-ε-caprolactone) diblock copolymer, PCL-b-PME_3CL. The same procedure was followed for the synthesis of PCL-*b*-PME_3CL with exeriment ratio [ε-CL]:[γ-ME_3CL]:[TBD]:[BnOH] = 45:55:1:1. ^{1}H NMR (500 MHz, $CDCl_3$) δ: 1.35-1.41 (m, 2H), 1.61-1.68 (m, 4H), 1.73-1.90 (m, 4H), 2.29-2.32 (t, 2H), 2.35-2.43 (m, 2H), 3.37 (s, 3H), 3.44-3.48 (m, 1H), 3.53-3.57 (m, 2H), 3.59-3.67 (m, 10H), 4.05-4.07 (t, 2H), 4.14-4.17 (m, 2H). ^{13}C NMR δ: 24.58, 25.54, 28.36, 29.08, 29.76, 33.09, 34.12, 59.01, 61.33, 64.15, 68.54, 70.54, 70.62, 70.72, 71.91, 71.94, 75.81, 173.46, 173.49, 173.54. SEC: Mn = 6000 gmol^{-1}, PDI = 1.38.

Procedures of critical micelle concentration determination, lower critical solution temperature measurement, reparation of empty micelles, and preparation of quercetin loaded micelles are shown in Supporting Information.

Conflicts of interest

There are no conflicts to declare.

Acknowledgements

Financial support from the Welch Foundation (AT-1740), National Science Foundation (CHE-1609880) is gratefully acknowledged. M. C. S. thanks the endowed chair support from the Eugene McDermott Foundation. This project was partially funded by the University of Texas at Dallas Office of Research through the Core Facility Voucher Program.

References

1. W. Xu, P. Ling and T. Zhang, *J Drug Deliv*, 2013, **2013**, 340315.
2. B. Reddy, H. K. Yadav, D. K. Nagesha, A. Raizaday and A. Karim, *Journal of nanoscience and nanotechnology*, 2015, **15**, 4009-4018.
3. D. Hwang, J. D. Ramsey and A. V. Kabanov, *Adv Drug Deliv Rev*, 2020, **156**, 80-118.
4. E. A. Rainbolt, K. E. Washington, M. C. Biewer and M. C. Stefan, *Polym. Chem.*, 2015, **6**, 2369-2381.
5. J. Hao, E. A. Rainbolt, K. Washington, M. C. Biewer and M. C. Stefan, *Current Organic Chemistry*, 2013, **17**, 930-942.
6. K. E. Washington, R. N. Kularatne, V. Karmegam, M. C. Biewer and M. C. Stefan, in *Stimuli Responsive Polymeric Nanocarriers for Drug Delivery Applications, Volume 1*, Elsevier, 2018, pp. 501-529.
7. Y. Xiao, M. Yuan, J. Zhang, J. Yan and M. Lang, *Current Topics in Medicinal Chemistry*, 2014, **14**, 781-818.
8. J. Yan, Z. Ye, M. Chen, Z. Liu, Y. Xiao, Y. Zhang, Y. Zhou, W. Tan and M. Lang, *Biomacromolecules*, 2011, **12**, 2562-2572.
9. P. Soltantabar, E. L. Calubaquib, E. Mostafavi, M. C. Biewer and M. C. Stefan, *Biomacromolecules*, 2020, **21**, 1427-1436.
10. J. Hao, Y. Cheng, R. U. Ranatunga, S. Senevirathne, M. C. Biewer, S. O. Nielsen, Q. Wang and M. C. Stefan, *Macromolecules*, 2013, **46**, 4829-4838.
11. S. Basu, D. R. Vutukuri and S. Thayumanavan, *Journal of the American Chemical Society*, 2005, **127**, 16794-16795.
12. E. N. Savariar, S. V. Aathimanikandan and S. Thayumanavan, *Journal of the American Chemical Society*, 2006, **128**, 16224-16230.
13. T. Liu, W. Tian, Y. Zhu, Y. Bai, H. Yan and J. Du, *Polymer Chemistry*, 2014, **5**, 5077-5088.
14. E. L. Calubaquib, P. Soltantabar, H. Wang, H. Shin, A. Flores, M. C. Biewer and M. C. Stefan, *Polymer Chemistry*, 2021, **12**, 3544-3550.
15. L. Wen, S. Zhang, Y. Xiao, J. He, S. Zhu, J. Zhang, Z. Wu and M. Lang, *Macromolecules*, 2020, **53**, 5096-5104.
16. R. Chen, Z. Xiang, Y. Xia, Z. Ma, Q. Shi, S. C. Wong and J. Yin, *Macromolecular Rapid Communications*, 2020, **41**, 2000206.
17. X.-h. Fu, Y.-n. Ma, J. Sun and Z.-b. Li, *Chinese Journal of Polymer Science*, 2016, **34**, 1436-1447.
18. J.-F. Lutz, K. Weichenhan, Ö. Akdemir and A. Hoth, *Macromolecules*, 2007, **40**, 2503-2508.
19. J.-F. Lutz, Ö. Akdemir and A. Hoth, *Journal of the American Chemical Society*, 2006, **128**, 13046-13047.
20. F. Hua, X. Jiang, D. Li and B. Zhao, *Journal of Polymer Science Part A: Polymer Chemistry*, 2006, **44**, 2454-2467.
21. L. Song, B. Zhang, E. Jin, C. Xiao, G. Li and X. Chen, *European Polymer Journal*, 2018, **101**, 183-189.
22. Y.-H. Kim, I. C. Kwon, Y. H. Bae and S. W. Kim, *Macromolecules*, 1995, **28**, 939-944.
23. Y. Zou, D. E. Brooks and J. N. Kizhakkedathu, *Macromolecules*, 2008, **41**, 5393-5405.
24. S. Chen, K. Wang and W. Zhang, *Polymer Chemistry*, 2017, **8**, 3090-3101.
25. M. Sahn, T. Yildirim, M. Dirauf, C. Weber, P. Sungur, S. Hoeppener and U. S. Schubert, *Macromolecules*, 2016, **49**, 7257-7267.
26. Q. Zhang, C. Weber, U. S. Schubert and R. Hoogenboom, *Materials Horizons*, 2017, **4**, 109-116.
27. K. Van Durme, H. Rahier and B. Van Mele, *Macromolecules*, 2005, **38**, 10155-10163.
28. E. Thormann, *Rsc Advances*, 2012, **2**, 8297-8305.
29. K. Sakota, D. Tabata and H. Sekiya, *The Journal of Physical Chemistry B*, 2015, **119**, 10334-10340.
30. P. O. Stănescu, I. C. Radu, C. Drăghici and M. Teodorescu, *Reactive and Functional Polymers*, 2020, **152**.
31. S. Saeki, N. Kuwahara, M. Nakata and M. Kaneko, *Polymer*, 1977, **18**, 1027-1031.
32. M. Bozorg, B. Hankiewicz and V. Abetz, *Soft Matter*, 2020, **16**, 1066-1081.
33. C. Zhang, H. Peng and A. K. Whittaker, *Journal of Polymer Science Part A: Polymer Chemistry*, 2014, **52**, 2375-2385.
34. Y. Zhang, S. Furyk, L. B. Sagle, Y. Cho, D. E. Bergbreiter and P. S. Cremer, *The Journal of Physical Chemistry C*, 2007, **111**, 8916-8924.
35. H. S. Yoo and T. G. Park, *Journal of controlled Release*, 2001, **70**, 63-70.
36. K. E. Washington, R. N. Kularatne, M. C. Biewer and M. C. Stefan, *ACS Biomaterials Science & Engineering*, 2018, **4**, 997-1004.
37. Y. Qiao, C. Zhan, C. Wang, X. Shi, J. Yang, X. He, E. Ji, Z. Yu, C. Yan and H. Wu, *Journal of Materials Chemistry B*, 2020, **8**, 8527-8535.
38. Y. Shi, M. J. van Steenbergen, E. A. Teunissen, L. s. Novo, S. Gradmann, M. Baldus, C. F. van Nostrum and W. E. Hennink, *Biomacromolecules*, 2013, **14**, 1826-1837.
39. K. E. Washington, R. N. Kularatne, J. Du, M. J. Gillings, J. C. Webb, N. C. Doan, M. C. Biewer and M. C. Stefan, *Journal of Polymer Science Part A: Polymer Chemistry*, 2016, **54**, 3601-3608.
40. E. A. Rainbolt, J. B. Miller, K. E. Washington, S. A. Senevirathne, M. C. Biewer, D. J. Siegwart and M. C. Stefan, *Journal of Materials Chemistry B*, 2015, **3**, 1779-1787.
41. G.-B. Jiang, D. Quan, K. Liao and H. Wang, *Carbohydrate Polymers*, 2006, **66**, 514-520.
42. L. Yang, Z. Zhao, J. Wei, A. El Ghzaoui and S. Li, *Journal of colloid and interface science*, 2007, **314**, 470-477.

43. H. Wang, F. Xu, Y. Wang, X. Liu, Q. Jin and J. Ji, *Polymer Chemistry*, 2013, **4**, 3012-3019.
44. Q. Li, W. Yao, X. Yu, B. Zhang, J. Dong and Y. Jin, *Colloids and Surfaces B: Biointerfaces*, 2017, **158**, 709-716.
45. S. S. Baghel, N. Shrivastava, R. S. Baghel, P. Agrawal and S. Rajput, *World J Pharm Pharmaceutical Sci*, 2012, **1**, 146-160.
46. M. Zhang, S. G. Swarts, L. Yin, C. Liu, Y. Tian, Y. Cao, M. Swarts, S. Yang, S. B. Zhang and K. Zhang, in *Oxygen transport to tissue XXXII*, Springer, 2011, pp. 283-289.
47. D. Xu, M.-J. Hu, Y.-Q. Wang and Y.-L. Cui, *Molecules*, 2019, **24**, 1123.
48. M. Ezzati, B. Yousefi, K. Velaei and A. Safa, *Life Sciences*, 2020, **248**, 117463.
49. M. Hashemzaei, A. Delarami Far, A. Yari, R. E. Heravi, K. Tabrizian, S. M. Taghdisi, S. E. Sadegh, K. Tsarouhas, D. Kouretas and G. Tzanakakis, *Oncology reports*, 2017, **38**, 819-828.
50. P. Maleki Dana, F. Sadoughi, Z. Asemi and B. Yousefi, *Cancer Cell International*, 2021, **21**, 1-9.
51. R. Baksi, D. P. Singh, S. P. Borse, R. Rana, V. Sharma and M. Nivsarkar, *Biomedicine & Pharmacotherapy*, 2018, **106**, 1513-1526.
52. A. Vafadar, Z. Shabaninejad, A. Movahedpour, F. Fallahi, M. Taghavipour, Y. Ghasemi, M. Akbari, A. Shafiee, S. Hajighadimi and S. Moradizarmehri, *Cell & bioscience*, 2020, **10**, 1-17.
53. S. Nathiya, M. Durga and D. Thiyagarajan, *International Journal of Pharmacy and Pharmaceutical Sciences*, 2014, 20-26.
54. A. Rauf, M. Imran, I. A. Khan, M. ur‐Rehman, S. A. Gilani, Z. Mehmood and M. S. Mubarak, *Phytotherapy Research*, 2018, **32**, 2109-2130.